Experimental Analysis of Combustion Instabilities on a combustor rig for Various Compositions of Alternative Fuels

Swapneel Roy
[1]Department of Mechanical Engineering, University of Sheffield
Sheffield, South Yorkshire, UK, S1 3JD

Bhupendra Khandelwal
[2]Department of Mechanical Engineering, University of Sheffield
Sheffield, South Yorkshire, UK, S1 3JD

Abstract

Today, the aviation industry faces numerous challenges in the energy sector. Depleting fossil fuels reserves, ever increasing consumption and crude oil price hike has escalated concerns over the supply security of petroleum derived Jet fuel. Also, stricter emissions legislation to preserve the environment and reduce CO_2 emissions has compelled the aviation industry to explore alternatives to current aviation Jet fuel. The advent of various synthetic and alternative fuels production has paved the way for aviation industry to test the compatibility of these fuels to the existing aero-derivative engines. Hence, it is vital to investigate the effect of these fuels on combustion instabilities. In this paper, the authors have investigated the effect of different compositions of alternative fuels on combustion dynamics and emissions when compared to Jet A-1. The fuels under investigation are Jet A-1, 100 percent Heavily Hydro-processed fuel from conventional source and their mixtures varied in percentage weight. Vibrational data were recorded for Spey can combustor rig for a range of AFRs. Significant deviation in vibration response was witnessed with different compositions of fuels for both the rigs. Gaseous emissions have been included to provide a wider perspective along with combustion dynamics.

1. Introduction

With the objective to meet stricter emissions legislations, gas turbine manufacturers developed Lean premixed (LP) combustion systems to reduce NOx, CO and THC emissions. The LP combustion systems such as Dry Low-Emissions Combustor (DLE) used in Trent 60 Aero-derivative gas turbine [1-2], introduce high levels of air to operate the engine at higher AFRs or leaner fuel mixtures to reduce the flame temperature, which is an exponential function of NOx formation rate [3]. But this development has encouraged the occurrence of combustion instabilities which are pre-dominant in lean mixtures of AFR.

Combustion instabilities are undesirable outcome of all Gas Turbine Engines. The pressure amplitude and velocity oscillations produces thrust oscillations, vibrations which can interfere with control system operation, heightened heat transfer, thermal stress to combustor liner, fluctuating mechanical loads [5].

These in turn encourages low/high cycle fatigue of system components and flashbacks [5]. At some operating conditions the combustion generates an externally audible tone at intolerable limits [6]. Also, pressure oscillations lead to significant hardware damage when they match resonant frequency of vibrations in mechanical components in gas turbine engines [6-7]. The damage/failure of combustor liner reroutes the compressor delivery air through the wall of the liner instead of premixers which changes the fuel-air distribution and mixing in the combustor [8]. Figure 1 showS the damage to combustor liner and burner assembly due to combustion instabilities.

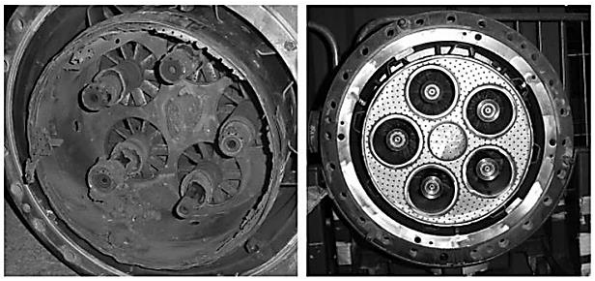

Figure 1: Failed burner assembly [8]

Rayleigh's criterion was the first contribution in this field of study postulated by Lord Rayleigh which described the conditions in which unsteady heat release adds energy to the acoustic field [4-5]. For instability condition to be satisfied the driving of oscillation must be greater than the damping of oscillations [4-5]

The above definition is numerically [5] given as:

$$R = \int_0^T p'(t)q(t)'dt$$

When R>0, Rayleigh's criterion is satisfied and the phase between heat addition and pressure oscillations $\varphi_{p'q'}<90^0$, where, R is Rayleigh's index, p' depicts fluctuation in pressure and q' depicts fluctuation in heat release.

Previous researches on combustion instabilities have indicated three mechanisms before determining the instability; a feedback system between the heat release rate and acoustic oscillation, a driving mechanism which depends upon the phase between heat release rate and acoustic oscillation, and damping of oscillations by viscosity, heat transfer and acoustic radiation [5]. Combustion can be said to have attained instability if driving of oscillations is greater than the damping of oscillations [5].

The fluctuations in equivalence ratio encourage the heat release oscillations which contribute to the feedback loop. The equivalence ratio fluctuations are exhibited in a frequency broadband by significantly higher harmonics in comparison to pressure oscillations which are exhibited at/near fundamental frequency [9]. Furthermore, it was later proved that the fluctuations in equivalence ratio, first generates variations in heat of reaction, flame speed and flame area, which in turn affects the heat release rate [10-11, 14].

2. Experimental Set-up

A re-commissioned Rolls Royce Spey can combustor rig was utilised to investigate the combustion instabilities and emissions of different fuels. The combustor rig

was installed at the end of the 6 inch atmospheric line, powered by an industrial fan which delivered air flow at a constant rate.

The Spey can combustor rig was provided by Rolls-Royce which housed a single can with a fuel spray nozzle and an igniter. This rig was reconditioned and restored prior to the experiments. The can combustor is placed in the housing which is tightly fit and the can is attached with a pin near the inlet to secure its position and avoid any clanking with the housing. Seven K-type thermocouples were installed at various locations as shown in figure 2. Two thermocouples were installed at the exhaust, four at the can wall and one at the inlet. One pressure transducer was installed at the inlet to read the inlet pressure.

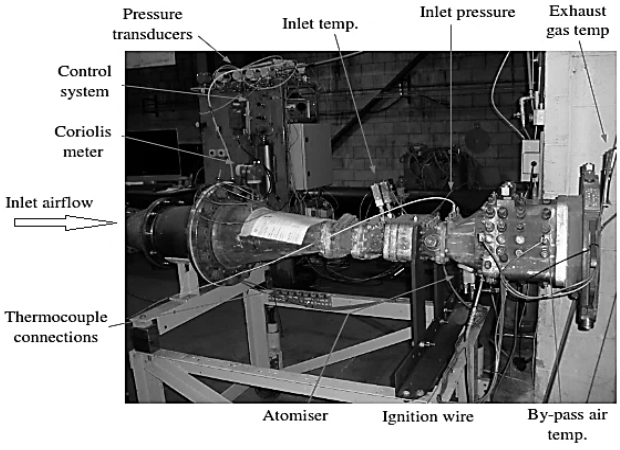

Figure 2: Spey rig showing installed sensors on the rig

The vibration of the combustor rig upon combustion was recorded with help of three miniature accelerometers mounted to the rig at three different locations as shown in the figure 3. Dytran's Low Impedance Voltage Mode accelerometers were operated with a current source (powered by 9V battery) delivering constant voltage of 11V.

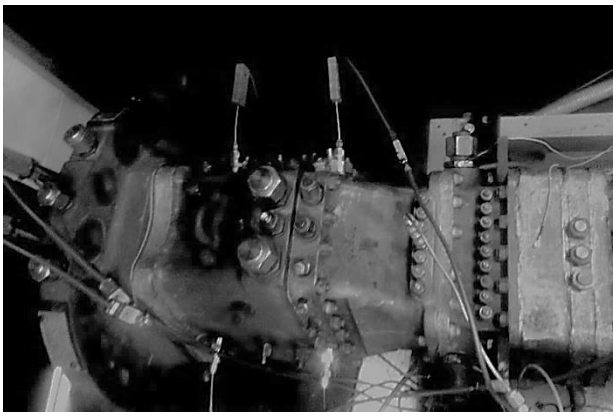

Figure 3: Installed Vibration analysers on the rig

The output of the current sources was connected to the DATAQ as three channels by three separate BNC cables which fed in milli-volt fluctuations and the corresponding amplitudes were recorded by the WinDAQ software. The sampling rate was set to 5000 samples per second which corresponded to 1666.67 Hz per channel. The sensitivity of the accelerometers at this frequency range corresponded to 10.52 mV/g. Figure 4 shows the flowchart of the signal acquisition.

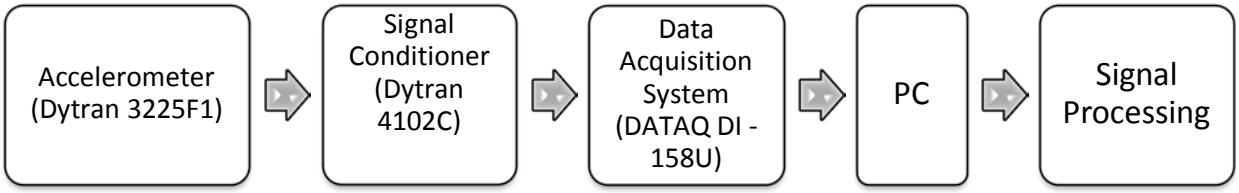

Figure 4: Signal Acquisition

Measurement of Emissions

Gaseous emissions such as CO, CO_2, NOX and THC were collected at the exhaust of the combustor rig and were sampled in Mobile Emissions Laboratory. The sampling port was not placed directly after the exhaust of the rig as it would inject fuel directly into the measuring instruments in an event of blowout or in process of fuel jettison. The sampling port was placed at the end of the conical tunnel and the position of the port was maintained at the same spot for all the tests.

A water cooled gaseous emissions probe mounted on the steel plate was utilised to supply sample to Sheffield University's Mobile Emissions Laboratory. Conditioned exhaust sample was introduced into the Mobile Emissions Laboratory through a ¼ inch heated line. The sample lines were maintained at 150±5°C as per ARP1256c [12], with a minimum bend radius of 10x the line diameter. Constant sampling flow rate (and system pressure) was maintained for the gaseous analysis equipment by using a metal bellows pump, with excess sample being exhausted through a back pressure regulator. Gaseous emissions (UHC, CO, CO_2 and NOx) were measured as per ARP1256c [12]. Table 1 tabulates the above description.

No.	Analyser/Unit	Gas
1	Routing Unit	------
2	FID	THC
3	CLD	NOx
4	NOx GEN	------
5	NDIR, Chiller	CO, CO_2
6	MAG	O_2
7	FTIR	THC

Table 1: Emission Analysers

The analysers were zeroed, and then spanned using appropriate gas concentrations just prior to the beginning of each experiment, with the zero and span drift established at engine shutdown. Instrument linearity and interference effects were assessed and corrected for as per the aerospace recommended practices (ARP1256 [12]). The experimental error associated with the measurement of emissions is estimated to be approximately ±2% of reading.

3. Operating conditions

The combustion conditions of an operational aircraft vary significantly on basis of flight speed and altitude, engine rpm and ambient conditions. It is highly unlikely to duplicate the complete flight envelope of combustion process with the existing set-up. The atmospheric line is capable of

delivering air mass flow rate to the Spey can-combustor rig between 0-0.47 Kg/s. Also due to restricted availability of time for the experiment, it was decided to operate the combustor with a fixed inlet air mass flow rate while varying the fuel flow to achieve a range of AFRs. Hence it was pre-dominantly essential in perspective of the combustor operation and atmospheric line restrictions to select a suitable air mass flow rate. A mass flow rate of 0.42 kg/s was chosen which falls well within the delivery range of industrial fan.

As the current aim of low NOx combustor requires that combustion take place in lean mixtures of AFR, an air mass flow rate of 0.42 Kg/s is sufficiently high to achieve lean mixtures allowing sufficient fuel flow for ignition stability. Taking air mass flow rate of 0.42 Kg/s, four AFRs are tabulated in Table 2 for a range of fuel flow. These four conditions, varying from a lean AFR to richer AFR, were maintained for all the fuels tested in this experiment.

Condition	**m_{air} kg/s)**	**Fuel flow (g/s)**		**AFR (mean)**
		Mean	***S.D.***	
1	0.42	2.5	±0.06	170
2	0.42	3.5	±0.06	120
3	0.42	4.5	±0.06	93
4	0.42	5.5	±0.06	75

Table 2: Selected AFRs

The fuel compositions and aromatic content are represented in table 3.

Fuels	Composition by % weight	Density (Kg/m3)	Aromatic content (% Weight)
Fuel 1	100% Jet A-1	799.8	≈18.2
Fuel 2	100% Heavily Hydro-processed fuel from conventional source	801.2	14.9
Fuel 3	85% Fuel 1and 15% Fuel 2	≈800	17.71
Fuel 4	65% Fuel 1and 35% Fuel 2	≈800	17.045
Fuel 5	60% Fuel 1and 40% Fuel 2	≈800	16.88
Fuel 6	50% Fuel 1and 50% Fuel 2	≈800	16.55

Table 3: Fuel compositions

4. RESULTS AND DISCUSSION

Analysis of Vibration Response of the combustor rig

The combustion instabilities of all fuels are represented in form of vibration response of combustor rig. The vibration response of the combustor rig on combustion of different fuels with varied aromatic content were recorded and their time domain signals were converted to frequency domain signals for better analysis of the results. The figures show distinct narrow band spikes and multiple resonances.

Figures 5-8 show the normalised power spectrum of vibration response (instability) of the rig for Fuel 1-6 at four different conditions. A general trend can be

observed where the leanest mixture of AFR (condition 1) shows relatively higher instability than the other conditions. As we progress toward lower AFRs (Richer mixtures) the instability decreases.

A leaner AFR would provide the flame with less volume of fuel droplets and the flame front would be weak (Lesser energy having lesser flame speed). The acoustic reflection on the flame would get increased interaction time to encourage further instabilities such as fuel feed line pressure changes contributing to the feedback loop.

Figures 5-9 also show that Fuel 2 has prolonged instability at all conditions due to higher fuel flow extinction limit. Fuel 2 shows relatively lower instability in LFD range (<50 Hz) and higher instability in IFD (50-1000 Hz). This trend is also seen in fuel 1 but with significant differences. The resonances of fuel 1 are highly damped in IFD range and are seen to have a relatively higher instability only till 100 Hz, whereas fuel 2 resonances are enhanced after 100 Hz.

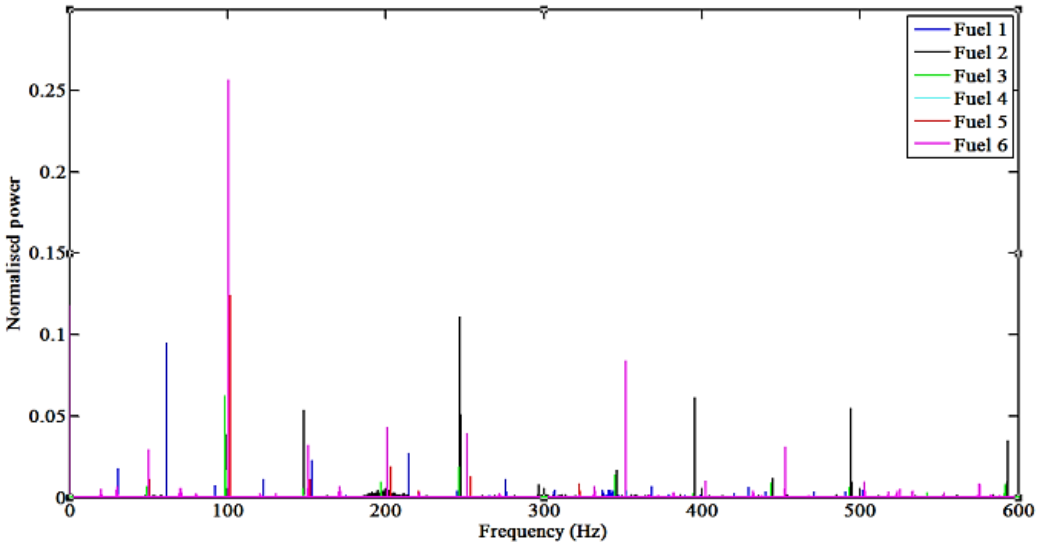

Figure 5: Normalised power spectrum at condition 1 for fuels 1-6

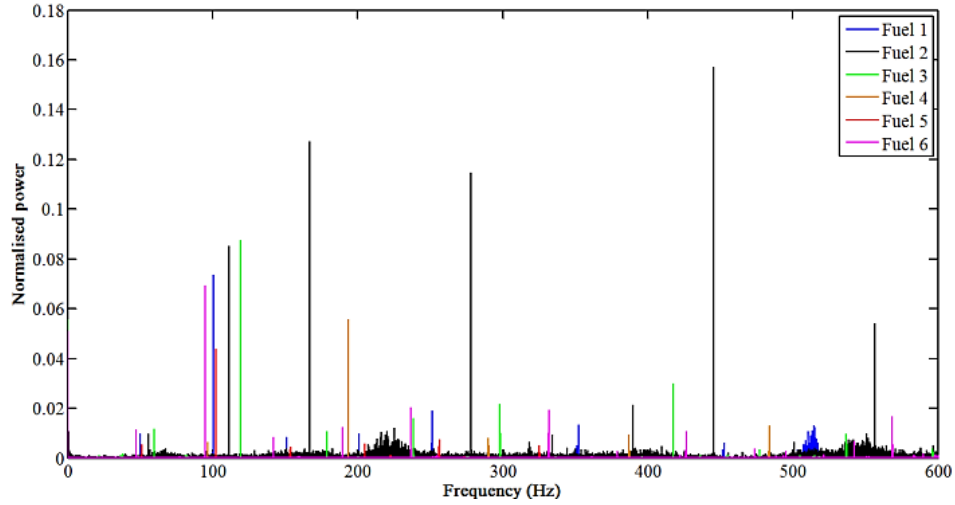

Figure 6: Normalised power spectrum at condition 2 for fuels 1-6

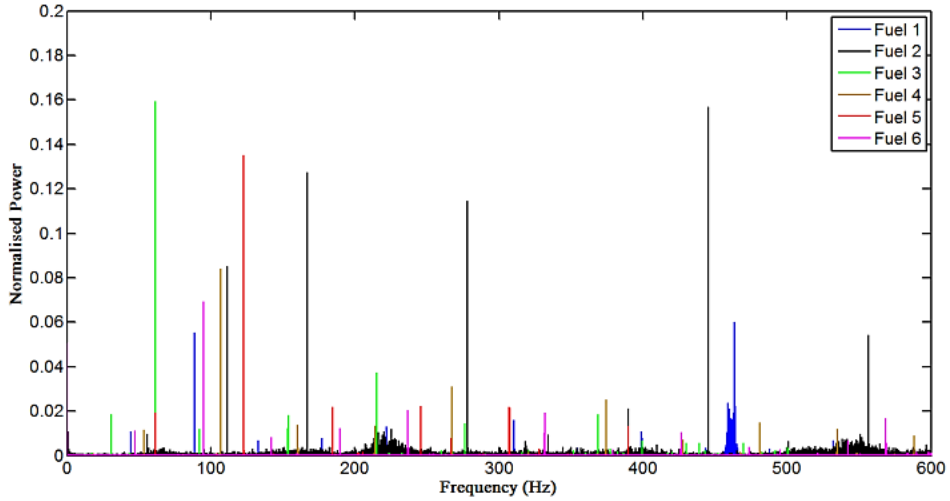

Figure 7: Normalised power spectrum at condition 3 for fuels 1-6

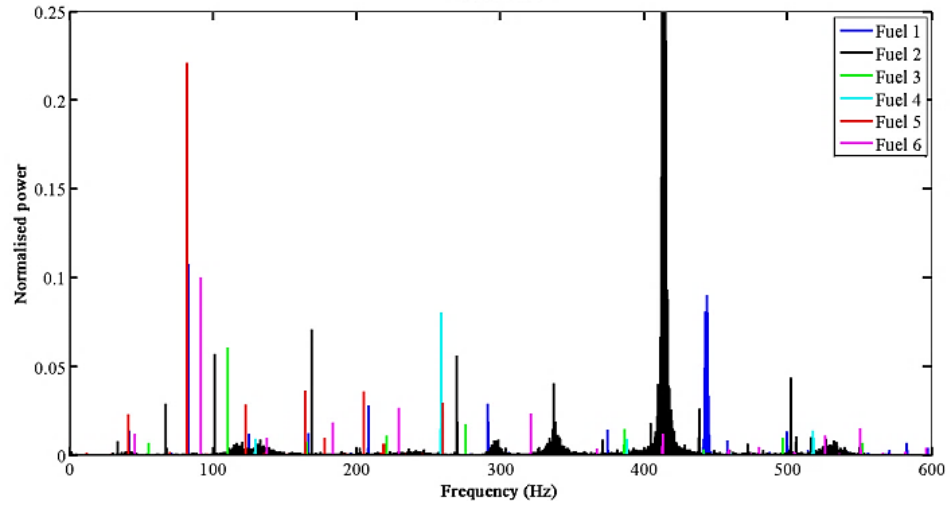

Figure 8: Normalised power spectrum at condition 4 for fuels 1-6

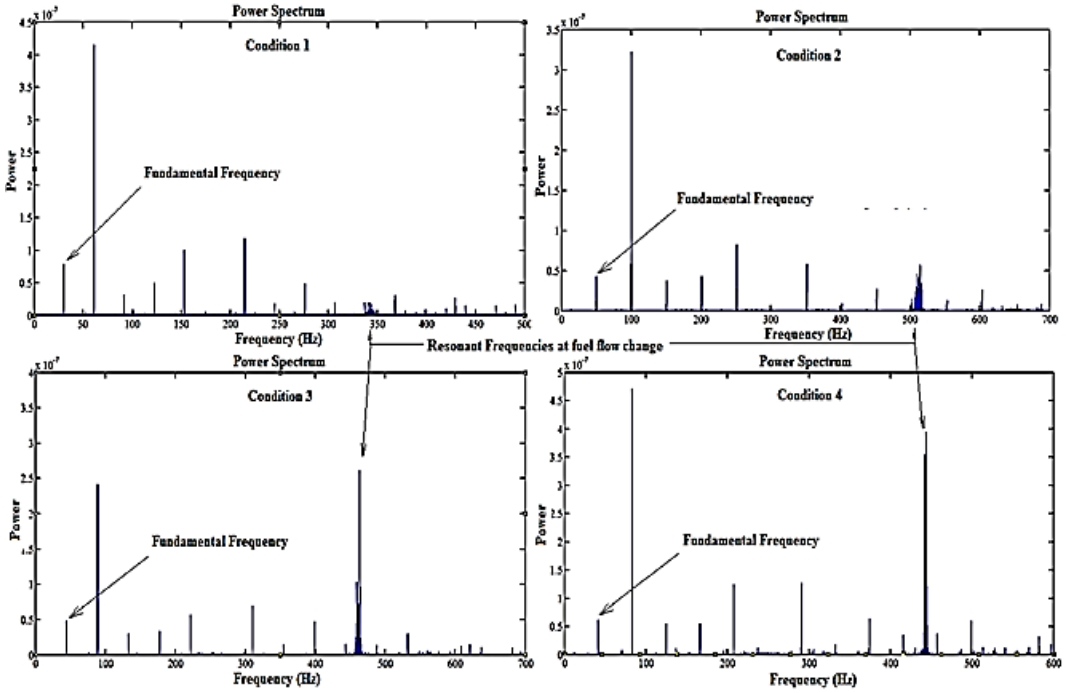

Figure 9: Power spectrum of vibration amplitude of combustor rig for fuel 1

Although fuel 1 and fuel 2 are from conventional sources, the reason for this deviation in response may be due to presence of different fuel components (or in varied percentage) present in the fuels as they come from different refinery process. The exact composition of these fuels is not accessible and hence no relation could be developed.

Fuel 3-6 are mixtures of varied percentage of fuel 1 and 2 (see table 3). The instability of these fuels does not follow a separate pattern but have close resemblance to the fuel 1 and fuel 2. The resemblance is relative to the dominant fuel of the mixture. Fuel 3 (mixture of 85% Jet A-1 and 15 % Shale) has close similarity to fuel 1 (100% Jet A-1) than fuel 2 in regard to frequency range characteristics discussed above. Fuel 3 also shows reduced instability after 100Hz. For decreasing fuel 1 percent content in a mixture, at condition 1, at 100 Hz, fuel 5 and fuel 6 have higher power in comparison to other fuels as seen in figure 5.

Figure 9 shows the power spectrum of Jet A-1 at four different conditions. The fundamental frequencies at condition 1-4 are 30.68 Hz, 50.32 Hz, 44.36 Hz and 41.59 Hz respectively. The fundamental frequency together with other resonant frequencies suggests that the vibrations occur in harmonics as the higher frequency resonances are multiples of the fundamental frequency. The second harmonic has the highest power for all conditions. The power spectrum of fuels 1-6 are observed to occur

in harmonics with one fundamental frequency. It is also noted that the sixth harmonic at all four conditions has the lowest power and the power of the resonant frequencies are highly damped in IFD region. The bundled spikes (resonances) occurring in the IFD region are due to sudden change of fuel flow from one condition to the other.

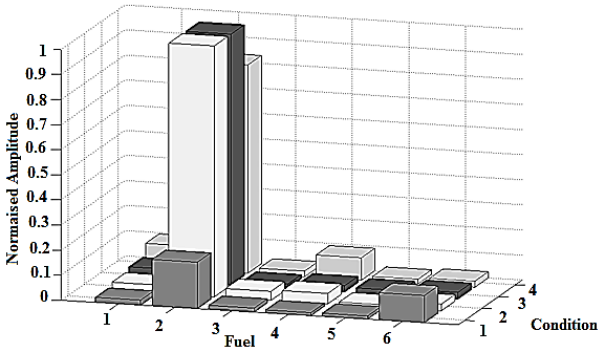

Figure 10: Normalised amplitude of fuels 1-6

Figure 10 shows the normalised amplitude of fuels 1-6. It is clearly seen that the fuel 2 has the maximum amplitude response of all the fuels. It is also observed that the blends of fuel 1 and 2 have lower instability than fuel 1 and 2 itself.

Gaseous Emissions

The gaseous emissions CO, CO_2, NOx, THC and O_2 were measured for the Spey can combustor rig for fuels 1-6. The comparison of the gaseous emissions is shown in figures 11-14.

CO emission is seen to increase from leaner to richer mixture of AFR in figure 11. Fuel 1 has higher CO emission in comparison to fuel 2 and its blends at all conditions. There is a decreasing trend for fuel 1 and fuel 2 blends. Fuel 2 and fuel 6 does not follow this trend as they had greater flame instability and were prone to irregular flame blow out due to higher fuel flow extinction limit.

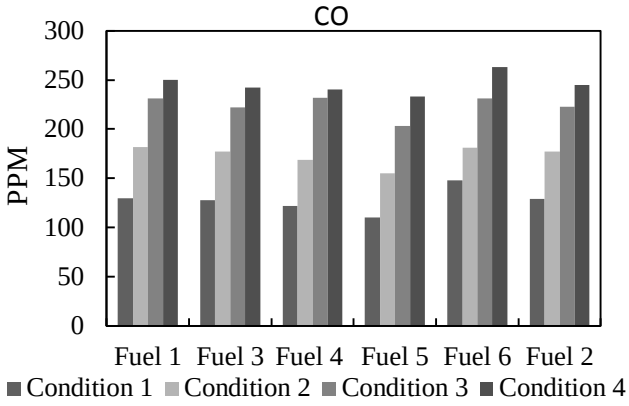

Figure 11: CO emission comparison of fuels

THC (Total hydrocarbons) showed decreasing trend from condition 1 to 4. THC follows an opposite trend to CO emissions as seen from figure 11 and figure 12.

CO_2 emissions are seen to increase with richer fuel mixtures (decreasing AFRs) as shown in figure 13. Fuel 1 produces higher CO_2 emissions than other mixtures of fuel 1 and fuel 2.

The NOx emission is function of flame temperature. Higher aromatic content fuels are seen to have greater NOx emissions as shown in figure 14. In general, there is a decreasing trend of NOx emissions for fuel 1, fuel 2 and their mixtures as decreasing aromatics reduces the flame temperature. As mentioned earlier, fuel 6 having greater flame instability, did not

fit this trend perfectly but had lower values than fuel 1.

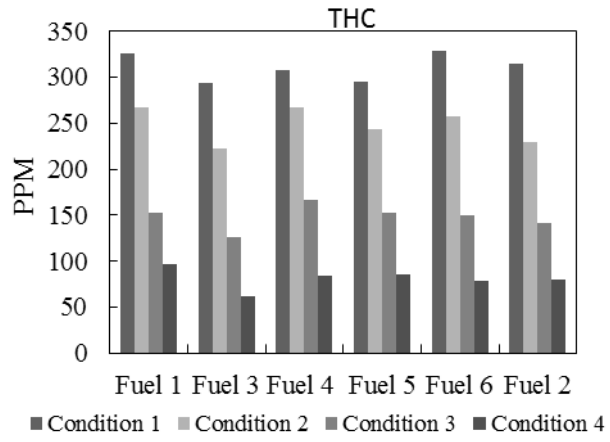

Figure 12: THC comparison

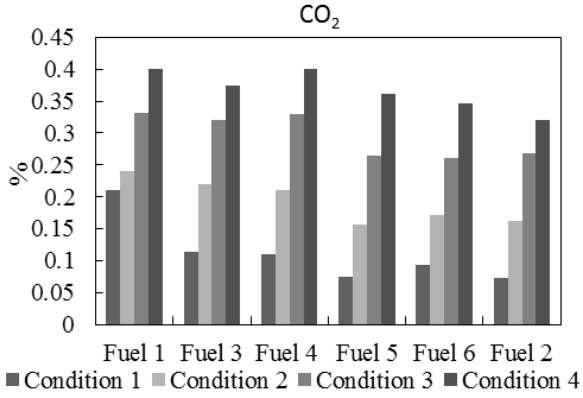

Figure 13: CO_2 emission comparison

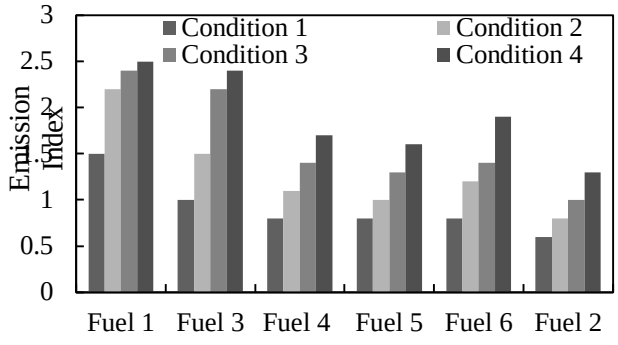

Figure 14: NOx comparison

References

1. Combustion Instability and its Passive Control: Rolls Royce Aeroderivative Engine Experience. Scarinci, T. 2005, Progress in Astronautics and Aeronautics, vol. 210, ed. T.C. Lieuwen and Vigor Yang, Pp 65-88.
2. Industrial Trent Combustor-Combustion Noise Characteristics. Scarinci, T, and Halpin, J H. 2000, Journal of Engineering for Gas Turbine and Power, vol. 122, No. 2, pp. 280-286.
3. Combustion Instabilities in Industrial Gas Turbines: Solar Turbines' Experience. Smith, K O, and Blust, J. 2005, Progress in Astronautics and Aeronautics, Vol. 210, ed. T.C. Lieuwen and Vigor Yang, pp 30-41.
4. The Theory of Sound. Rayleigh, J S W. 1945, vol. 2, Dover, New York.
5. Combustion Instabilities: Basic Concepts. Zinn, B T, Lieuwen, T C. 2005, Progress in Astronautics and Aeronautics, vol. 210, ed. T.C. Lieuwen and Vigor Yang, pp 3-26.
6. Incorporation of Combustion Instability Issues into Design Process: GE Aeroderivative and Aero Engines Experience. Mongia, H C, Held, T J, Hsiao, G C, Pandalai, R P. 2005, Progress in Astronautics and Aeronautics, vol. 210, Ed. T.C. Lieuwen and Vigor Yang, pp 43-64.
7. Dynamics and Stability of Lean Premixed Swirl Stabilized Combustion. Huang, Y, Yang, V. 2009, Progress in

Energy and Combustion Science vol. 35, pp. 293–364.
8. Monitoring Combustion Instabilities: E.ON Uk's Experience. Goy, C J, James, S R, Rea, S. 2005, Progress in Astronautics and Aeronautics, vol. 210, Ed. T.C. Lieuwen and Vigor Yang, pp 163-175.
9. Measurement of Equivalence Ratio Fluctuation and Its Effect on Heat Release during Unstable Combustion. Lee, J G, Kim, K, and Santavicca, D A. 2000, Proceedings of the Combustion Institute, vol. 28, pp. 415–421.
10. Laminar Premixed Flame Response to Equivalence Ratio Oscillations. Cho, J H, Lieuwen, T. 2005, Combustion and Flame, vol. 140, pp. 116–129.
11. A Mechanism of Combustion Instability in Lean Premixed Gas Turbine Combustor. Lieuwen, T, Torres, H, Johnson, C, Zinn, B T. 2001, Transactions of the ASME, Journal of Engineering for Gas Turbines and Power Vol. 123, DOI: 10, 1115/l .1339002.
12. ARP1256c. Procedure for the Continuous Sampling and Measurement of Gaseous Emissions from Aircraft Turbine Engines. SAE International 2006.
13. Gas Turbine Combustion, Lefebvre, A W., McGraw-Hill Series in Energy Combustion and Environment, 1983.
14. Comparison of Vibrations and Emissions of Conventional Jet Fuel with Stressed 100% SPK and Fully Formulated Synthetic Jet Fuel, Khandelwal, B., Roy, S., Lord, C., Blakey, S., Aerospace 1 (2), 52-66